Crack detection and analyses using resonance ultrasonic vibrations in full-size crystalline silicon wafers

A. Belyaev, O. Polupan, W. Dallas, S. Ostapenko,[a] and D. Hess
Nanomaterials and Nanomanufacturing Research Center, University of South Florida, 4202 East Fowler Avenue, Tampa, Florida 33620

J. Wohlgemuth
BP Solar International LLC, Frederick, Maryland 21703

(Received 13 April 2005; accepted 8 February 2006; published online 15 March 2006)

An experimental approach for fast crack detection and length determination in full-size solar-grade crystalline silicon wafers using a resonance ultrasonic vibrations (RUV) technique is presented. The RUV method is based on excitation of the longitudinal ultrasonic vibrations in full-size wafers. Using an external piezoelectric transducer combined with a high sensitivity ultrasonic probe and computer controlled data acquisition system, real-time frequency response analysis can be accomplished. On a set of identical crystalline Si wafers with artificially introduced periphery cracks, it was demonstrated that the crack results in a frequency shift in a selected RUV peak to a lower frequency and increases the resonance peak bandwidth. Both characteristics were found to increase with the length of the crack. The frequency shift and bandwidth increase serve as reliable indicators of the crack appearance in silicon wafers and are suitable for mechanical quality control and fast wafer inspection. © *2006 American Institute of Physics*. [DOI: 10.1063/1.2186393]

The photovoltaic industry, with crystalline silicon as a dominant segment, is expanding rapidly to meet growing renewable energy demands all over the world. One of the current technological problems is to identify and eliminate sources of mechanical defects such as thermo-elastic stress and cracks leading to the loss of wafer integrity and ultimate breakage of as-grown and processed Si wafers and cells. The problem is of increased concern as a result of the current strategy of reducing wafer thickness down to 100 μm.[1] Cracks generated during wafer sawing or laser cutting can propagate due to wafer handling and solar cell processing (e.g., phosphorous diffusion, antireflecting coating, front and back contact firing, and soldering of contact grid). It is recognized that development of a methodology for fast in-line crack detection and control is required to match the throughput of typical production lines. At this time, there are several experimental methods, which address the problem of crack detection in silicon. They include scanning acoustic microscopy,[2] ultrasonic lock-in thermography,[3] and millimeter wave techniques.[4]. Crack can be also accessed using laser-induced ultrasonic pulses.[5] None of these methods are suitable in their present form for rapid in-line crack diagnostics of as-grown and processed Si wafers. In solar cell manufacturing, in-line control requires methods which can achieve measurement times close to 2 s/wafer to match a throughput of a production line.

In this letter, we propose utilizing an alternative approach based on the recently developed resonance ultrasonic vibrations (RUV) methodology, which was successfully applied to monitor elastic stress in multicrystalline silicon solar-grade wafers.[6]

In the RUV method, ultrasonic vibrations of a tunable frequency and adjustable amplitude are applied to the silicon wafer. Ultrasonic vibrations are generated in the wafer using an external piezoelectric transducer in the frequency range from 20 to 90 kHz. The transducer contains a central hole allowing a reliable vacuum coupling between the wafer and transducer by applying a small ($\sim$50 kPa) negative pressure to the backside of the wafer. The vibrations propagate into the wafer from the transducer and form standing acoustic waves at resonance frequencies, which can be analyzed with a broadband ultrasonic probe. Using a frequency sweep (f-scan) through a particular resonance mode, the RUV system provides accurate measurements of the resonance frequency, the maximum vibration amplitude, and the bandwidth (BW) of the resonance curve using the ultrasonic probe. In the present design, the broadband ultrasonic probe measures the longitudinal vibration mode characteristics by contacting the edge of the wafer with a sensor controlled contact force. The ac signal from the probe is measured using standard lock-in technique and f-scans are analyzed by WINDOWS based software. The system is described in more details elsewhere.[6] We also used the *HS*1000 *HiSPEED*™ scanning acoustic microscope (SAM) by Sonix Inc. for surface morphology and structural (bulk) integrity evaluation of the wafers.[7]

A set of 20 identical 125 mm × 125 mm pseudosquare shaped (100) oriented Czochralski silicon (Cz-Si) wafers were chosen for this study. This shape represents one of the accepted photovoltaic industry standards. The wafers were as-grown with a nominal thickness of 0.035 cm. All wafers were initially screened by SAM for structural integrity. The SAM maps have been measured with a 100 μm step and no periphery or bulk cracks have been observed within this accuracy. Using the RUV vibrations technique frequency scans of the longitudinal vibrations from 20 to 85 kHz were measured on all wafers. A typical full range acoustic spectrum obtained on one of the wafers is shown in Fig. 1. In the frequency spectrum, we observed a set of distinctive resonance modes, which are consistently reproduced from wafer to wafer in terms of the maximum amplitude (±10%), fre-

[a]Author to whom correspondence should be addressed; electronic mail: ostapenk@eng.usf.edu

 © 2006 American Institute of Physics
Downloaded 13 Apr 2006 to 131.247.13.43. Redistribution subject to AIP license or copyright, see http://apl.aip.org/apl/copyright.jsp

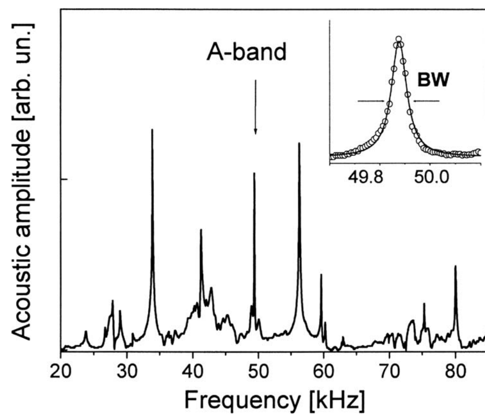

FIG. 1. Full range ultrasonic frequency spectrum obtained on 125 mm × 125 mm Cz-Si wafer. Inset shows the *A*-mode experimental data (open circles) and fitting Lorentz approximation (solid line). Line bandwidth (BW) parameter is shown by arrows.

quency position (±10 Hz) and BW (±10 Hz). One of these resonance modes assigned hereafter the *A* mode is observed at frequency f=49 930±20 Hz. We suggest tracking f-scan characteristics of the *A* mode as a means of crack detection and control in the wafers. A primary criterion for the *A*-mode selection is a noticeable clearance from the neighbor peaks to avoid their overlapping and interference, which would reduce the accuracy of the mode analyses. As seen from Fig. 1 (inset), the *A* mode is indeed a standalone narrow peak with BW=90±10 Hz.

We emphasize that the *A*-mode frequency scan and shape analyses can be measured with sufficient signal-to-noise ratio (>20 dB) in a time as short as 3 s. This obviously makes the RUV approach feasible and attractive for potential implementation as an in-line wafer quality control module. The other important feature of the RUV method is that according to vibration theory, the resonance frequencies of the longitudinal vibration modes are independent of the wafer thickness (h), in contrast to the flexural vibrations, which are proportional to $h^{3/2}$.[8] This is especially beneficial in the multicrystalline silicon (mc-Si) ribbon wafers, which may have significant (up to 20%) thickness variations across the wafer, as well as from wafer to wafer, which can be measured accurately using the SAM technique.[7] We tested this statement by varying the Cz-Si wafer's thickness between 100 and 350 μm. The frequency of the principle vibration modes observed in the RUV scans show slight (1.6%) high-frequency shift with reduced wafer thickness, which can be attributed to stress increase as was previously observed in mc-Si ribbon wafers.[6] It should be noted that every resonant peak shown in Fig. 1 represents a certain longitudinal vibration mode, both symmetrical and asymmetrical. Other type of vibrations (e.g., flexural modes) has lower frequencies and has to be excited in a different manner.[9,10] In this letter, we concentrate on the *A* mode only. The solid line in the insert in Fig. 1 shows the numeric approximation of the experimental frequency sweep for the *A* mode. This approximation is obtained with the Lorentz function and the following parameters have been extracted: peak resonance frequency, f_0, and bandwidth, BW.

To introduce or engineer cracks with different sizes, we have taken a few wafers and formed the crack by scribing the wafer edge with a diamond pin. As expected, the cracks originate at the spot of the diamond application and are oriented along ⟨110⟩ crystallographic directions. The length of each engineered crack has been measured using SAM in the precision mode with a 10 μm step. The SAM image of one of these cracks is presented in Fig. 2(a). After careful SAM study, the RUV measurements on the wafers with cracks have been carried out and the frequency spectra of the *A* mode recorded. In Fig. 3, we demonstrate the *A*-mode spectra in wafers with different crack sizes. Clearly, the *A*-mode resonance frequency decreases with increasing crack length (also see Δf line in inset in Fig. 3). We noticed that the vibration spectrum of the wafer with the 28 mm crack is nonsymmetrical indicating sufficient nonlinearity of the wafer vibrations induced by the crack. In addition, the *A*-mode BW increases with crack length. We were able to clearly detect mm size cracks by assessing *A*-mode line shift and broadening. Specifically, a 3 mm crack is exhibited as 160 Hz shift and an 8% increase BW. We estimate that the RUV approach offers submillimeter crack length sensitivity in Cz-Si wafers.

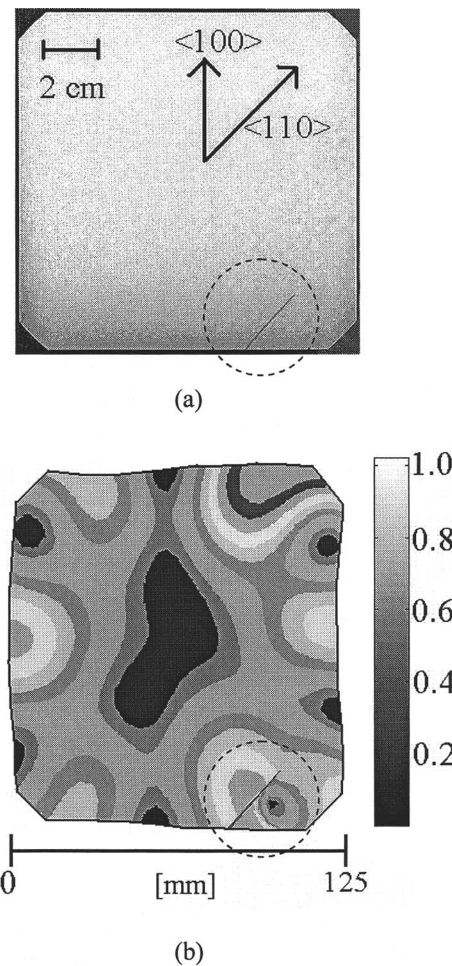

FIG. 2. (a) Scanning Acoustic Microscopy image of the 125 mm × 125 mm Cz-Si wafer with introduced 28 mm periphery crack. (b) Vibration mode at 51 052 Hz obtained with finite element analysis calculations on the wafer with identical crack. The color bar represents relative values of the acoustic amplitude of the water.

The downward shift with crack length of the low-frequency flexural resonance modes was previously observed in circular shaped membranes.[11] The decrease of the *A*-mode frequency and its dependence on crack length observed in our study are consistent with finite element analysis (FEA).[12] The wafer is modeled as a 125×125 mesh, with the size of

Downloaded 13 Apr 2006 to 131.247.13.43. Redistribution subject to AIP license or copyright, see http://apl.aip.org/apl/copyright.jsp

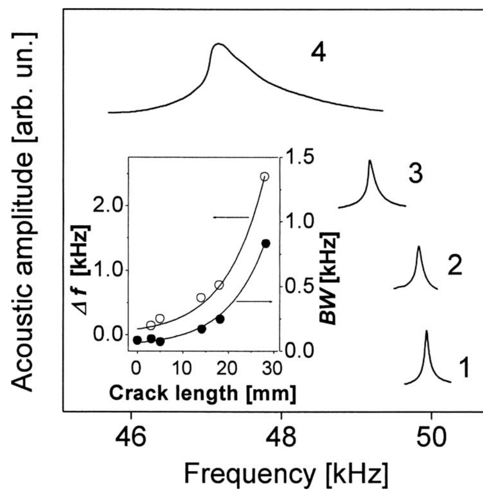

FIG. 3. The *A*-mode spectra of a non-cracked Cz-Si wafer (1), and wafers with different ⟨110⟩ crack lengths: (2) 3.0 mm, (3) 18 mm, and (4) 28 mm. The insert shows the dependence of the *A*-mode frequency shift and bandwidth variation vs crack length.

individual elements being 1.25 mm × 1.25 mm. The pseudosquare wafers are modeled with isotropic eight-node planar elements with a Young's modulus of 167 GPa, a Poisson's coefficient of 0.3, and a density of 2.329×10^3 kg/m^3. The resonance frequencies up to 100 kHz and respective mode shapes of the free edge longitudinal vibrations of the shell were calculated. We concentrated on the frequency shift of the vibration mode at $f_0 = 51\,052$ Hz, which is closest to the experiment value for the *A* mode. Figure 2(b) shows a calculated profile of the vibration mode on the wafer with identical geometry as the experimental Cz-Si wafers containing a 28 mm periphery crack. The crack size and location are identical to the experimental values. The FEA shows a decrease in frequency shift with increased crack length, which supports our experiment. However, calculated values show a much larger frequency shift than observed experimentally. Specifically, in a case of 28 mm crack FEA predicts a shift of the *A*-mode peak at 6900 Hz (experimental data is $\Delta f = 2\,450$ Hz). It was initially thought that one possibility for this difference could be the increase in damping in the test wafers with increased crack length. However, even though the BW is proportional to damping, and therefore damping increases with crack length by about 1 order of magnitude in the tests presented, the actual damping levels associated with the longitudinal *A* mode are very low for all test wafers. Therefore, the increased damping with crack length does not notably decrease the modal frequency. To clarify this, the damping level can be quantified by the modal damping ratio $\zeta = \mathrm{BW}/2f_0$ in terms of BW and modal undamped natural frequency f_0. The modal damped natural frequency is related to undamped natural frequency and the damping ratio as $f_d = f_0\sqrt{1-\zeta^2}$.[13] Since the damping ratio for the cracked wafers range from 0.001 to 0.01, the modal damped and undamped natural frequencies are essentially equal. A more likely possibility for the difference between experimental and numerical results is that the FEA models an ideal crack without contact elements and contact forces. Contact forces in a crack are inevitable when the test wafer is subjected to vibratory excitation. Such forces would tend to provide some stiffness and thereby result in the smaller frequency shift observed experimentally compared to the wafer model simulations without contact forces. Contact elements can be introduced in the FEA. Such efforts are currently in progress and are expected to improve the model and therefore our estimation capabilities.

This work presented an experimental methodology using the resonance ultrasonic vibrations technique to detect cracks in crystalline silicon substrates for solar cells. A shift of the resonant frequency and line broadening of the longitudinal vibration mode versus crack length has been shown. These dependences clearly demonstrate a direct relation of the extracted parameters on crack length. The RUV system allows fast data acquisition and analyses matching the throughput of solar cell production lines. The probable mechanism of the observed effect is a decrease in wafer stiffness affecting the vibration mode frequency with the mm length peripheral crack.

The work was partially supported by the NREL Subcontract Nos. AAT-2-31605-06 and ZDO-2-30628-03.

[1] J. Wohlgemuth, M. Narayanan, R. Clark, T. Koval, S. Roncin, M. Bennett, D. Cunningham, D. Amin, and J. Creager, *Proceedings Conference Record of the 31st IEEE Photovoltaic Specialist Conference* (IEEE, New York, 2005, p. 123.
[2] A. Belyaev, O. Polupan, S. Ostapenko, D. Hess, and J. Kalejs, Department of Energy "Solar Energy Technologies" Program Review Meeting, Denver, October 2004.
[3] P. Rakatoniania, O. Breitenstein, M. H. Al Rifai, D. Franke, and A. Schneider, *Proceedings of the 194th European Photovoltaic Solar Energy Conference and Exhibition*, Paris, 7–11 June 2004 (in press).
[4] Y. Ju, Y. Ohno, H. Soyama, and M. Saka, *Proceedings of the 16th World Conference on Non-Destructive Tesing*, Montreal, Canada, August–September 2004.
[5] Q. Shan and R. J. Dewhurst, Appl. Phys. Lett. **62**, 2649 (1993).
[6] A. Belyaev, O. Polupan, S. Ostapenko, D. Hess, and J. Kalejs, Semicond. Sci. Technol. **21**, 254 (2006).
[7] T. Moore, *Proceedings International Symposium on Testing and Failure Analysis*, 1989, pp. 61–67.
[8] R. D. Blevins, *Formulas for Natural Frequencies and Mode Shapes* (Krieger, 2001), pp. 233–290.
[9] S. Ostapenko and I. Tarasov, Appl. Phys. Lett. **76**, 2217 (2000).
[10] A. Belyaev, I. Tarasov, S. Ostapenko, S. Koveshnikov, V. A. Kochelap, and A. E. Belyaev, ECS Proc. **17**, 660 (2000).
[11] H. Huang and C. C. Ma, J. Sound Vib. **236**, 637 (2000).
[12] I. Shames and C. Dym, *Energy and FEA in Structural Mechanics* (McGraw–Hill, New York, 1985), pp. 520–530.
[13] D. J. Ewins, *Modal Testing: Theory. Practice and Application*, 2nd ed. (Research Studies, England, 2000).

Downloaded 13 Apr 2006 to 131.247.13.43. Redistribution subject to AIP license or copyright, see http://apl.aip.org/apl/copyright.jsp